

**Analysis of diffractive  $pd \rightarrow Xd$  and  $pp \rightarrow Xp$  interactions and test of the finite-mass sum rule\***

Y. Akimov, L. Golovanov, S. Mukhin, and V. Tsarev<sup>†</sup>

*Joint Institute for Nuclear Research, Dubna, Union of Soviet Socialist Republics*

E. Malamud, R. Yamada, and P. Zimmerman<sup>‡</sup>

*Fermi National Accelerator Laboratory, Batavia, Illinois 60510*

R. Cool, K. Goulios, and H. Sticker

*Rockefeller University, New York, New York 10021*

D. Gross, A. Melissinos, D. Nitz, and S. Olsen<sup>§</sup>

*University of Rochester, Rochester, New York 14627*

(Received 1 June 1976)

Cross sections for the reaction  $pp \rightarrow Xp$  in the diffraction dissociation region, extracted from the recently reported precise Fermilab data on  $pd \rightarrow Xd$ , are compared with results from Fermilab and CERN ISR. The  $M_X^2$ ,  $t$ , and  $s$  dependences are discussed and the first-moment finite-mass sum rule is tested.

Recently, a precise measurement of the inclusive inelastic process

$$p + d \rightarrow X + d \tag{1}$$

in the region  $50 < p_{1ab} \leq 400$  GeV/c,  $0.03 < |t| \leq 0.12$  (GeV/c)<sup>2</sup>, and  $1.4 \text{ GeV}^2 < M_X^2 \leq 0.11 p_{1ab}$  was reported.<sup>1,2</sup> This range of  $M_X^2$  includes the resonance as well as the triple-Regge region<sup>3</sup> (TR region:  $M_X^2 \gg m_p^2$  and  $M_X^2/s \leq 0.1$ ). In this report, we analyze the  $pd$  results and we test the first-moment finite-mass sum rule<sup>4</sup> (FMSR).

Our analysis is performed on  $pp \rightarrow Xp$  cross sections extracted from the  $pd \rightarrow Xd$  data using factorization. By comparing the extracted  $pp \rightarrow Xp$  results with existing data we show that factorization holds to a good approximation. In any case, since the reduction to  $pp \rightarrow Xp$  cross sections involves division by a function of  $t$  only, our conclusions about the  $s$  and  $M_X^2$  dependence of the differential cross sections and about the validity of the FMSR are very insensitive to uncertainties in the extraction procedure.

**I. FACTORIZATION AND EXTRACTION OF  $pp \rightarrow Xp$  CROSS SECTIONS**

The  $pd \rightarrow Xd$  measurement was performed at Fermilab using an internal deuterium gas jet target. Elastic  $pd$  scattering was also studied<sup>5</sup> in the same  $p_{1ab}$  and  $t$  range. The elastic cross section factorizes approximately like  $(d\sigma/dt)^{pd} \approx (d\sigma/dt)^{pp} F_d(p_{1ab}, t)$ , where  $F_d(p_{1ab}, t)$  is the coherence factor defined as

$$F_d(p_{1ab}, t) = \left[ \frac{\sigma_T^{pd}}{\sigma_T^{pp}}(p_{1ab}) \right]^2 |S(t)|^2. \tag{2}$$

Here,  $\sigma_T^{pd(pp)}$  is the  $pd(pp)$  total cross section and

$S(t)$  is the deuteron form factor. In the region of small  $|t|$ , the data are reasonably well described by

$$|S(t)|^2 = e^{b_0 t + c t^2} \tag{3}$$

with<sup>5</sup>  $b_0 = 26.4 \pm 0.2$  (GeV/c)<sup>-2</sup> and  $c = 62.3 \pm 1.1$  (GeV/c)<sup>-4</sup>. Over the  $p_{1ab}$  range of the  $pd$  experiment, the factor  $(\sigma_T^{pd}/\sigma_T^{pp})^2$  is approximately constant and has the value<sup>6</sup> of 3.6 to within better than 2% accuracy. Thus, the coherence factor takes the form

$$F_d(t) \equiv F_d(50 < p_{1ab} < 400, |t| < 0.12) \approx 3.6 e^{26.4 t + 62.3 t^2}. \tag{4}$$

Assuming that the inelastic cross section factorizes in the same way as the elastic,

$$\frac{d^2\sigma}{dt dM_X^2}(pd \rightarrow Xd) = \left[ \frac{d^2\sigma}{dt dM_X^2}(pp \rightarrow Xp) \right] F_d(t) \tag{5}$$

one may then obtain cross sections for the reaction

$$p + p \rightarrow X + p \tag{6}$$

by dividing the measured cross sections for  $pd \rightarrow Xd$  by the elastic coherence factor. If the Glauber-type corrections for inelastic scattering are comparable to the corrections for elastic scattering ( $\approx 10\%$ ), this procedure is expected to yield the correct cross sections for  $pp \rightarrow Xp$ , including the values of the slope parameter, to within better than  $\sim 10\%$ .

Factorization was successfully tested<sup>1</sup> in the  $M_X^2 < 4$  GeV<sup>2</sup> region for  $|t| = 0.025$  (GeV/c)<sup>2</sup> and  $p_{1ab} = 180$  and 275 GeV/c. In Fig. 1, we compare the extracted  $pp \rightarrow Xp$  cross sections for  $p_{1ab} = 275$

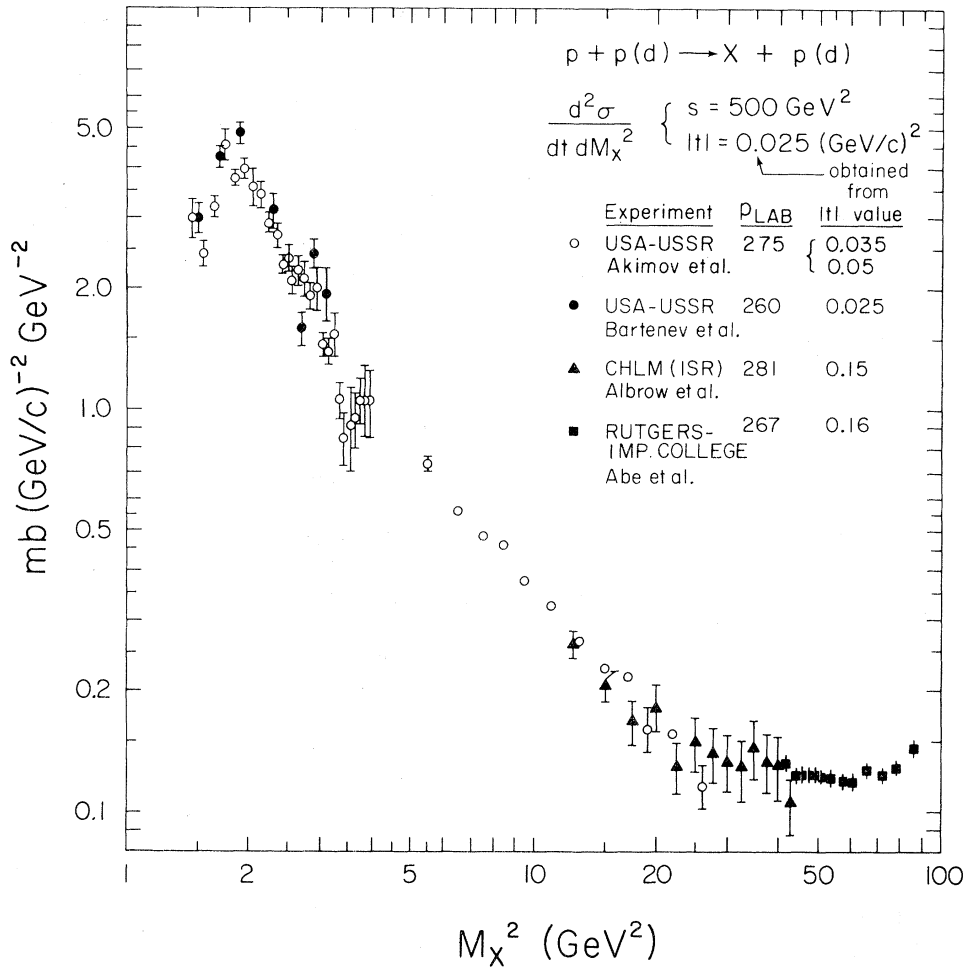


FIG. 1. Differential cross sections for  $pp \rightarrow Xp$  vs  $M_X^2$  for  $s \sim 500 \text{ GeV}^2$  and  $|t| = 0.025 \text{ (GeV/c)}^2$ , obtained from the listed  $|t|$  values using slopes given in the references. For the extrapolation of the CHLM collaboration (CERN, Holland, Lancaster, Manchester) and Rutgers-Imperial College data a slope of  $6 \text{ (GeV/c)}^{-2}$  was used.

$\text{GeV/c}$  and  $|t| = 0.025 \text{ (GeV/c)}^2$  with data from Fermilab<sup>7,8</sup> and CERN ISR,<sup>9</sup> where the points of Refs. 8 and 9 have been obtained from the measured cross sections at  $|t| = 0.15$  and  $0.16$ , respectively, by extrapolation using a slope of  $6 \text{ (GeV/c)}^{-2}$ . The agreement at low as well as high values of  $M_X^2$  is good within the experimental error of  $\sim \pm 10\%$ . The peaking of the cross section at low  $M_X^2/s$  is striking and the  $1/M_X^2$  behavior in the region  $5 \text{ GeV}^2 \lesssim M_X^2 \lesssim 0.05s$  is apparent.

## II. $M_X^2$ , $t$ , AND $s$ DEPENDENCE OF EXTRACTED $pp \rightarrow Xp$ CROSS SECTIONS

In the resonance region,  $M_X^2 < 5 \text{ GeV}^2$ , the  $M_X^2$  distributions of the extracted  $pp$  cross sections exhibit structure,<sup>1</sup> with a prominent broad enhancement centered at  $M_X^2 \approx 1.9 \text{ GeV}^2$  and a smaller

peak at  $M_X^2 \approx 2.8 \text{ GeV}^2$  probably to be identified with the  $N^*(1688)$  state. A still smaller bump may be present at  $M_X^2 \approx 3.7 \text{ GeV}^2$ . For  $M_X^2 > 5 \text{ GeV}^2$ , the cross sections at fixed  $s$  behave as  $1/M_X^2$ . The  $t$  distributions for fixed  $M_X^2$  are exponential<sup>1,2</sup> (see Fig. 2) with no sign of a turnover down to values of  $|t| \approx 0.03 \text{ (GeV/c)}^2$ . The slope parameter  $b(M_X^2)$  seems to be a function only of  $M_X^2$  independent of  $p_{\text{lab}}$ . In the resonance region,  $b(M_X^2)$  falls very rapidly from the value of  $\sim 20 \text{ (GeV/c)}^{-2}$  at  $M_X^2 \sim 1.9 \text{ GeV}^2$  to the average value<sup>2</sup> of  $6.5 \pm 0.3 \text{ (GeV/c)}^{-2}$  for  $M_X^2 \geq 5 \text{ GeV}^2$ .

Figure 3(a) shows  $b(M_X^2)$  versus  $M_X^2$  for  $p_{\text{lab}} = 275 \text{ GeV/c}$ . Figure 3(b) shows the differential cross section at  $t = 0$  multiplied by  $M_X^2$ , obtained by extrapolating the data at higher  $|t|$  values<sup>1,2</sup> using the slopes in Fig. 3(a). The  $M_X^2$  distributions of  $b(M_X^2)$  and of  $M_X^2(d^2\sigma/dt dM_X^2)_{t=0}$  have a

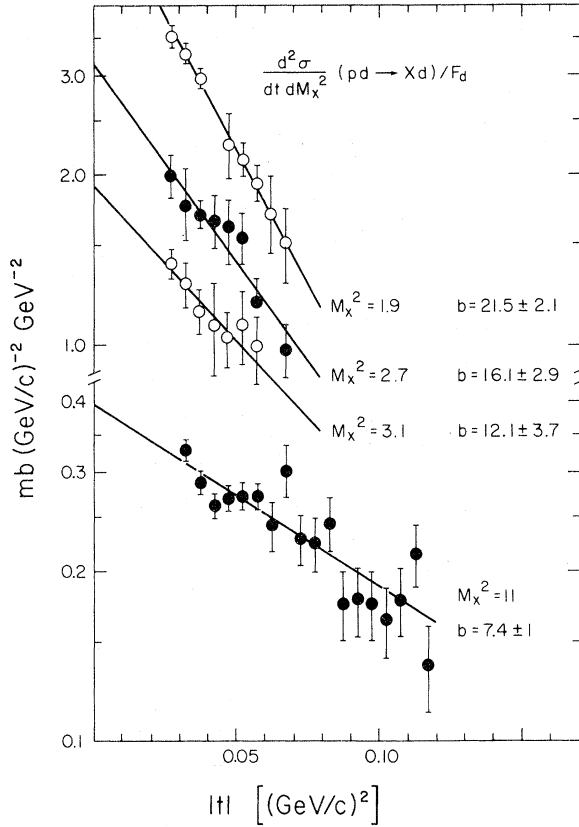


FIG. 2. Differential cross sections vs  $t$  for  $pp \rightarrow Xp$ , extracted from  $pd \rightarrow Xd$ , at  $p_{\text{lab}} = 275$  GeV/c, for  $M_X^2 = 1.9, 2.7, 3.1$ , and  $11$  GeV $^2$ .

very similar shape. Dividing the values of  $M_X^2$  ( $d\sigma/dt dM_X^2$ ) $_{t=0}$  in Fig. 3(b) by the values of the slopes in Fig. 3(a) yields  $M_X^2$  times the integral over  $t$  of the differential cross sections  $M_X^2(d\sigma/dM_X^2)$  shown in Fig. 3(c). Within the errors,  $M_X^2(d\sigma/dM_X^2)$  is approximately constant all the way down to  $M_X^2 \sim 1.7$  GeV $^2$ , where it starts dropping towards the pion threshold at  $M_X^2 \approx 1.15$  GeV $^2$ . Thus, the prominent low-mass enhancement at  $M_X^2 \sim 1.9$  GeV $^2$  observed at small fixed  $t$  values appears to be a manifestation of the increased value of the slope parameter. The cross section for the production of a mass,  $d\sigma/dM_X^2$ , follows the simple  $1/M_X^2$  behavior for all masses within the range of the  $pd$  experiment including the resonance region.

The extracted  $pp \rightarrow Xp$  cross sections in the high-mass region show a non-negligible energy dependence. An adequate fit of the differential cross section in this region is given by $^2$

$$\frac{d^2\sigma}{dt dM_X^2} = \frac{A(1+B/p_{\text{lab}})}{M_X^2} b_0 e^{b_0 t}, \quad (7)$$

where  $A = 0.54 \pm 0.02$  mb,  $B = 54 \pm 16$  GeV/c, and  $b_0 = 6.5 \pm 0.3$  (GeV/c) $^{-2}$ , where the uncertainties include a  $\pm 3\%$  normalization uncertainty. It is remarkable that this formula also describes well the average behavior of the cross section in the resonance region provided  $b_0$  is replaced by  $b(M_X^2)$  of Fig. 3(a).

In the kinematic region of the data, the inclusive cross section is expected to be described theoretically by the triple-Regge formula $^3$

$$\frac{d^2\sigma}{dt d\nu} = \frac{1}{s^2} \sum_{ijk} G_{ijk}(t) \left(\frac{s}{\nu}\right)^{\alpha_i(t) + \alpha_j(t)} \nu^{\alpha_k(0)}, \quad (8)$$

where  $\nu = M_X^2 - m_p^2 - t$  is the crossing-symmetric variable, the  $G_{ijk}(t)$  are the triple-Regge couplings, and the  $\alpha_i(t)$  are the Regge trajectories. Because the isospin of the deuteron is zero, only zero-isospin  $i$  and  $j$  trajectories can contribute to the triple-Regge expansion for reaction (1), excluding, for example,  $\pi\pi R$  and  $\pi\pi P$  couplings, which appear to contribute non-negligibly to  $pp \rightarrow Xp$ .

Ignoring for the moment the energy dependence of the data, the fitted result (7) shows that at each energy the  $\nu$  dependence is compatible with a pure triple-Pomeron coupling, for which Eq. (8) simplifies to

$$\frac{d^2\sigma}{dt d\nu} = \frac{G_{PPP}(t)}{\nu} \left(\frac{s}{\nu}\right)^{2\alpha' t}. \quad (9)$$

From Eqs. (9) and (7) we find that in the limit of  $s \rightarrow \infty$   $G_{PPP}(t) = (3.3 \pm 0.16)e^{(4.9 \pm 0.5)t}$  where we have used $^{10}$   $\alpha' = 0.278$  (GeV/c) $^{-2}$ .

To account for the energy dependence of the data in the TR formalism, we must add one or more energy-dependent terms to Eq. (9), for example an  $RRR$  term. A good fit to the data is obtained with  $PPP$ ,  $RRR$ , and  $PPR$  terms. The result, using  $\alpha'_R = 1$  (GeV/c) $^{-2}$  and fixing the slope at  $5$  (GeV/c) $^2$ , is

$$\begin{aligned} G_{PPP}(t) &= (3.20 \pm 0.36)e^{5t}, \\ G_{RRR}(t) &= (74 \pm 30)e^{5t}, \\ G_{PPR}(t) &= (1.00 \pm 0.63)e^{5t}, \\ \chi^2 &= 34.6/28 \text{ degrees of freedom.} \end{aligned} \quad (10)$$

An equally good fit is obtained with only the  $PPP$  and  $RRR$  terms, in which case the triple-Pomeron coupling is larger by 17%. However, the fit presented above is closer to satisfying the finite-mass sum rule, as will be shown below.

### III. TEST OF THE FMSR

The first-moment finite-mass sum rule states that, $^4$  at fixed  $t$ ,

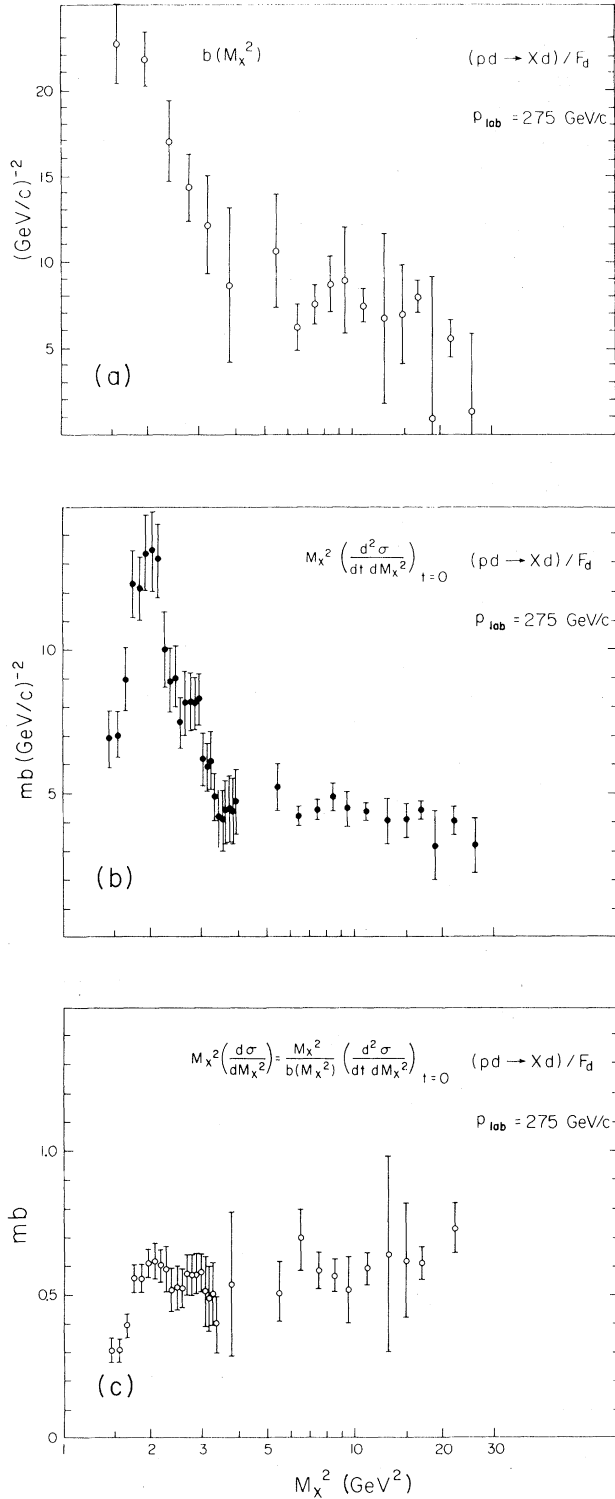


FIG. 3. Values for  $pp \rightarrow Xp$  vs  $M_X^2$ , extracted from  $pd \rightarrow Xd$  at 275 GeV/c. (a) The slope parameter,  $b(M_X^2)$ . (b)  $d^2\sigma/dt dM_X^2$  multiplied by  $M_X^2$  and extrapolated to  $t=0$  using  $b(M_X^2)$ . (c) Values of (b) above, divided by values of (a):  $M_X^2(d\sigma/dM_X^2)$ .

$$|t| \frac{d\sigma_{e1}}{dt} + \int^N \nu \frac{d^2\sigma}{dt d\nu} d\nu = \int^N \nu \left( \frac{d^2\sigma}{dt d\nu} \right)_{\text{TR}} d\nu, \quad (11)$$

where  $d\sigma_{e1}/dt$  is the differential elastic scattering cross section,  $(d^2\sigma/dt d\nu)_{\text{TR}}$  is the fit to the inelastic cross section in the TR region smoothly extrapolated to  $\nu=0$ , and  $N$  is any  $\nu$  corresponding to an  $M_X^2$  lying between resonances. For fixed  $t$ ,  $d\nu = dM_X^2$ . Figure 4 shows (i) the values of  $\nu d^2\sigma/dt dM_X^2$  versus  $M_X^2$  derived from the  $pd$  data<sup>1,2</sup> at 275 GeV/c and  $|t|=0.035$  (GeV/c)<sup>2</sup>, (ii) the experimental value of  $|t|d\sigma_{e1}/dt$  (derived from the  $pd$  data of Ref. 5) represented as a Gaussian-shaped area for illustrative purposes and, (iii) the fit to the data in the high-mass region of  $\nu(d^2\sigma/dt dM_X^2)_{\text{TR}}$  with the simple form of Eq. (9) extrapolated to  $M_X^2 = m_p^2$ , represented by the solid curve at the constant value of 3.1 mb (GeV/c)<sup>-2</sup>. The sum of the areas under (i) and (ii), representing the left-hand side of Eq. (11), equals the area under the solid curve representing the right-hand side of Eq. (11), to within the 3% normalization uncertainty. Thus, with the simple parametrization (9) of the high-mass data, the FMSR is satisfied to a high degree of accuracy. The validity of this rule for other  $t$  values within the range of the  $pd \rightarrow Xd$  experiment is equally good.

If one requires that the triple-Regge parametrization, Eq. (8), fit the high-mass data,<sup>2</sup> as well as the low-mass<sup>1</sup> and elastic scattering data<sup>5</sup> via the FMSR, Eq. (11), one obtains more accurate values for the TR couplings:

$$\begin{aligned} G_{PPP}(t) &= (2.91 \pm 0.25)e^{5t}, \\ G_{RRR}(t) &= (122 \pm 15)e^{5t}, \\ G_{PPR}(t) &= (1.00 \pm 0.14)e^{5t}, \\ \chi^2 &= 43.4/29 \text{ degrees of freedom.} \end{aligned} \quad (12)$$

We believe that the values of  $G_{PPP}(0)$  and  $G_{PPR}(0)$  obtained here are reliable, whereas the value of  $G_{RRR}(0)$  is quite sensitive to the inclusion of other  $s$ -dependent terms such as  $G_{RRP}(0)$ .

A number of other TR analyses of previously available  $pp \rightarrow Xp$  data have been reported.<sup>3,11</sup> For example, the authors of Ref. 11 report values of the TR couplings which were determined by fitting the high-energy, high-mass data while constraining the solutions to agree with lower energy, low-mass data through FMSR. Their best solution has nonzero  $PPP$ ,  $RRR$ ,  $PPR$ , and  $RRP$  couplings which, if reduced by about 10%, fit the high-mass  $pd \rightarrow Xd$  data well. The result of their solution No. 1 is  $G_{PPP}(0) = 2.63$ ,  $G_{RRR}(0) = 18.1$ ,  $G_{PPR}(0) = 4.42$ , and  $G_{RRP}(0) = 31.6$  which should be compared with our results (10) and (12). Their

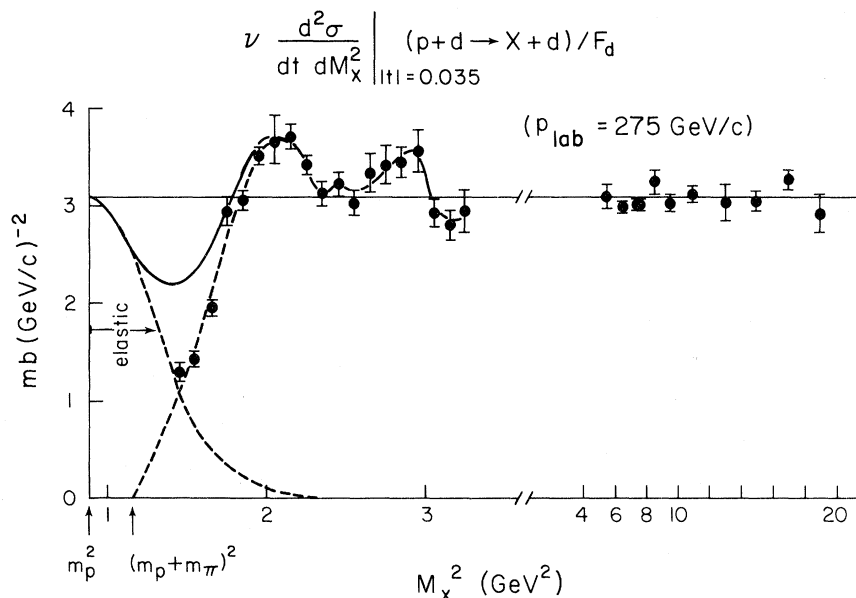


FIG. 4. Test of the first-moment FMSR: Values of  $\nu(d^2\sigma/dt dM_x^2)$  vs  $M_x^2$  for  $p_{\text{lab}}=275$  GeV/c and  $|t|=0.035$  (GeV/c)<sup>2</sup>.

value for  $G_{PPP}$  is somewhat smaller than our result, primarily because of the presence of a larger  $PPR$  term.

The tight correlation among the fitted parameters makes it difficult to extract a unique set of triple-Regge couplings. The new low-mass, high-energy deuterium data<sup>1</sup> provide an additional con-

straint for the determination of these couplings. Our fit (12) was constrained to satisfy the new data via the FMSR, while that of Ref. 11 fails to do so by about 40%.

We wish to thank Dr. Vladimir Rittenberg for many useful discussions.

\*Work supported in part by the U. S. Energy Research and Development Administration under Contracts No. E(11-1)-2232A and No. E(11-1)-3605, and by the U. S. S. R. State Committee for Atomic Energy

†Present address: P. N. Lebedev Institute, Moscow, U. S. S. R.

‡Present address: Louisiana State University, Baton Rouge, La. 70803.

§Work supported in part by a fellowship from the Alfred P. Sloan Foundation.

<sup>1</sup>Y. Akimov *et al.*, Phys. Rev. Lett. **35**, 763 (1975).

<sup>2</sup>Y. Akimov *et al.*, Phys. Rev. Lett. **35**, 766 (1975).

<sup>3</sup>See, for example, D. P. Roy and R. G. Roberts, Nucl. Phys. **B77**, 240 (1974), and references therein.

<sup>4</sup>A. I. Sanda, Phys. Rev. D **6**, 280 (1972); M. B. Einhorn, J. Ellis, and J. Finkelstein, *ibid.* **5**, 2063 (1972).

<sup>5</sup>Y. Akimov *et al.*, Phys. Rev. D **12**, 3399 (1975).

<sup>6</sup>A. S. Carroll *et al.*, Phys. Lett. **61B**, 303 (1976).

<sup>7</sup>V. Bartenev *et al.*, Phys. Lett. **51B**, 299 (1974).

<sup>8</sup>K. Abe *et al.*, Phys. Rev. Lett. **31**, 1527 (1973).

<sup>9</sup>M. G. Albrow *et al.*, Nucl. Phys. **B72**, 376 (1974).

<sup>10</sup>V. Bartenev *et al.*, Phys. Rev. Lett. **31**, 1088 (1973).

<sup>11</sup>R. D. Field and G. C. Fox, Nucl. Phys. **B80**, 367 (1974).